

## Granular convection driven by shearing inertial forces

G. M. Rodríguez-Liñán and Y. Nahmad-Molinari\*

*Instituto de Física, Universidad Autónoma de San Luis Potosí, Álvaro Obregón 64, 78000, San Luis Potosí, Mexico*

(Received 10 June 2005; published 12 January 2006)

Convection velocity measurements in vertically vibrated granular materials are presented. The convection velocity close to the walls grows quadratically with the difference between the maximum and critical, or excess, amplitude  $A_e$  (proposed as a dynamic parameter to describe related problems) and it is shown numerically that the average bed-bottom relative velocity during the distancing between them, grows linearly with the squared  $A_e$  as well. This is interpreted as the signature of an inertial shearing force or momentum transfer proportional to the bed-container relative velocity, acting mainly during the bed-plate distancing part of each cycle which leads to the formation of the convective flux.

DOI: [10.1103/PhysRevE.73.011302](https://doi.org/10.1103/PhysRevE.73.011302)

PACS number(s): 45.70.-n

### I. INTRODUCTION

Vertical shaking in granular materials induces heaping and large scale convective motion of the bed. Industrial processes dealing with dry granular materials as in the case of pharmaceuticals leads in many cases to granular segregation that could be, for example, Brazil-nut-problem-like or Oyama's drumlike segregation [1]. In the best case, this phenomenon ends in a full lot of rejected pills, but in the worst, could cause lethal overdoses or subdoses of the active principle. On casting iron, very hard erosion and deformation of polystyrene molds is produced during the compaction of the sand bed due to the convective fluxes induced by the shaking process, causing a hard economic impact in the automotive industry. Convection may either cause or diminish segregation in vibrated systems in such a way that some processes can be bothered or helped by it.

Nevertheless, granular convection has been studied using particle image velocimetry [2], magnetic resonance imaging [3], positron emission tracking [4], and high speed photography methods [2,5], the underlying mechanism that produces this instability has remained undeveloped. Several hypotheses have been suggested to explain the onset of convection going from granular temperature gradients [6], friction with the walls and, density gradients up to shear banding [7]. Moreover, simple models for granular convection based on probabilistic considerations [8] have been put forward in order to explain the radial and axial velocity profiles observed experimentally in cylindrical cells [9]. However, there is not a clear experimental proof for any of the aforementioned driving mechanisms or how they are related to heaping, which is produced and maintained by convection itself [10]. Gallas and co-workers have shown, using molecular dynamics simulations [10] that interparticle shear as well as wall-particle shear forces can induce convection or heaping if the wall-particle shear is turned on or off, respectively. On their numerical experiments, they found a resonance of the convection speed close to the walls for a certain frequency and for three different exciting amplitudes.

A physical picture of the problem shared by some authors [11–13] is focused on the shear stress exerted by the walls during the ascension or distancing part of a single shaking cycle. It is mainly in this part of the cycle when most of the horizontal shear is relaxed, producing decompaction on the outermost shell of the granulate [12], some authors focus on this decompaction process and attribute the convecting or streaming mode as driven by density or buoyant effects [4,11,14]. Others [5] claim that the shock, or compaction wave, induces the observed convection and suggest that the kinetic energy at landing may be a more pertinent parameter to describe the phenomenon.

Inertial forces are important to explain the ascension of a large intruder within a column of small beads subjected to vertical vibration, phenomenon known as the Brazil nut problem (BNP) [15]. The report of a nonmonotonic behavior of the intruder rise times as a function of density was reported as early as 2001 [16] and was finally understood in 2004 [17] as an overlap of inertia and convective drag forces. Nevertheless, friction has been suggested as the driving mechanism behind the development of the convective flux in their experiments, it has never been proved experimentally. In this paper, we show that the average relative velocity between the bed and the plate during the distancing is the appropriate dynamic parameter which measures the strain of the granulate, per cycle, exerted by the inertial force of the shear stress against the walls.

It will be fruitful to clarify *a priori* the two main different vertical excitation regimes for a granular material being tapping and continuous shaking. In the first, the system is excited by a single sinusoidal cycle followed by a stand-by period during which the granulate is allowed to relax before a second cycle starts. In the second, a continuous sinusoidal excitation of frequency  $\omega$  is fed to the granulate and, if the frequency is low enough, the bed shall have time to relax as in the tapping regime. On the contrary, if the frequency is high enough, the excitation will be exerted before the grains have formed an isostatic net of stresses (relaxed bed) leading to a dynamically loose packing or a fluidized bed. In other words, there is a chain of stresses formation-time or relaxation-time characteristics of each system which defines a boundary between the solidlike and the fluidlike behavior in granular materials. On one hand, we can use a classical

\*Corresponding author. Electronic address: [yuri@ifisica.uaslp.mx](mailto:yuri@ifisica.uaslp.mx)

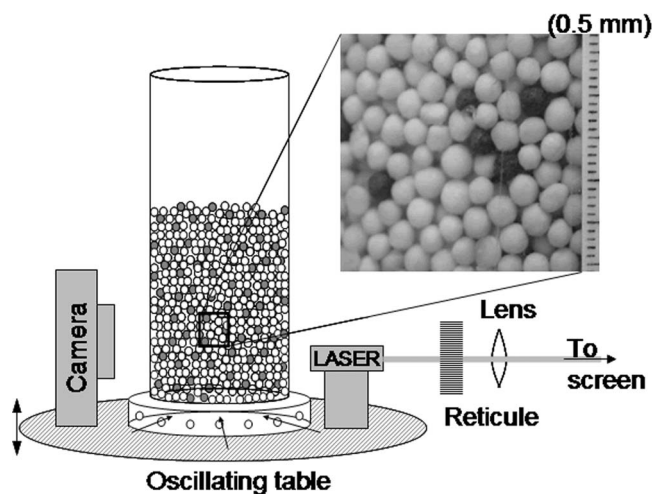


FIG. 1. Schematic diagram of the experimental setup showing the container mounted on top of a vibratory table and on a platform which allows the air to flow through the bottom of the cell. The reticule and lens are mounted on a table fixed to the laboratory. A picture of the granulate as seen by the digital camera shows the size of the grains in comparison with the scale at the right (0.5 mm).

mechanics approach—as in the case of the BNP—but on the other hand, hydrodynamic effects appear—as normal buoyancy or sinkage in the reverse BNP [17]—and the natural tool to use in this regime should be fluid mechanics. For very large excitations, the motion of the particles is not correlated anymore with the movement of the exciting element and we have a granular gas where kinetic theory is more appropriate to describe the collective behavior of our system.

## II. EXPERIMENTAL SETUP

Our experimental setup consists of a cylindrical 17-cm-high and 8-cm-diameter plexiglass cell with porous bottom, placed on top of a vibratory table fed by a sinusoidal signal from a Hewlett-Packard 33120A function generator. The cell is filled up to 9 cm height with 2.2 mm (average diameter) tapioca starch balls. This granular medium consists in spheroidal (circularity of 0.83) polydisperse [coefficient of variation (CV)=0.45%] particles of 0.57 g/cc density and a restitution coefficient close to 0.20. A small percentage of these “spheres” were dyed with permanent black ink to allow us to track them by digitally recording the convective flux close to the walls. To do this, a digital camera using a macro lens and recording at 30 frames per second was placed on the vibrating plate and the videos were loaded for posterior analysis. Care was taken in balancing the system in order to achieve acceleration uniformity on the entire plate. The bottom of the container was made porous by drilling a large number of holes and fixing a mesh to avoid particles to escape. These holes allow the air to easily penetrate from the lower part of the container diminishing the pressure gradient that is formed across the granulate when it is launched. In Fig. 1, a schematic diagram of the experimental setup is shown.

In order to determine how the convective flux depends on the shaking parameters—amplitude and frequency—the first

was measured directly by mounting a laser diode on the plate and projecting a reticule image of 0.32 mm interline spacing fixed to a static table in the lab. It was projected at a distance of about 5 m from the reticule in order to clearly count the number of lines spanned by the laser during the plate oscillation. On top of that, two small piezoelectric devices were mounted on the plate. The first configured as an accelerometer supported on a ring and with a ball bearing attached to it and the second glued on the bottom of the cell to probe the instantaneous load exerted by the granulate. This last piezoelectric element allows us to measure real times of flight starting not at the time the acceleration reaches  $g$  but at the time when the granulate loses contact with the container’s bottom, once the static frictional force exerted by the granulate on the walls has been surpassed. We have tested this piezoelectric element without any granular load and no appreciable signal is obtained, this means that it actually is not working as an accelerometer in the absence of load.

## III. RESULTS AND DISCUSSION

Let us consider a bed of granular material within a container under harmonic vertical vibration in which the container’s position described from the laboratory’s frame of reference is given by  $z_0 = A \sin \omega t$  then, the instantaneous velocity and acceleration are  $\dot{z}_0 = A\omega \cos \omega t$  and  $\ddot{z}_0 = -A\omega^2 \sin \omega t$ , respectively. For our purpose, it will be useful to determine the position, velocity, and acceleration of a material point as it is seen from the frame of reference of the oscillating plate for times after which the granulate lifts off from the plate. First let us define the critical amplitude,  $A_c = g/\omega^2$ , as the amplitude corresponding to the maximum acceleration of the plate equals  $g$ . For a fixed frequency and just above  $A_c$ , a particle placed on top of the plate will start to lose contact with it in each cycle, while below this critical value, the particle will remain in contact and no relative motion nor convection can occur. Then, for an arbitrary amplitude  $A$ , we will call the excess amplitude,  $A_e$ , to the difference  $A_e = A - A_c$ . Another important quantity to determine is the time,  $t_{to}$ , at which particles take off from the container’s bottom (or take-off time). Thus,  $t_{to}$  is obtained solving  $g = -A\omega^2 \sin \omega t$  for  $t$ , that is, when the net acceleration on the granulate is zero, giving

$$t_{to} = \frac{1}{\omega} \arcsin\left(\frac{g}{A\omega^2}\right) = \frac{1}{\omega} \arcsin\left(\frac{A_c}{A}\right). \quad (1)$$

Our experiments were performed in a frequency range from 5 to 15 Hz in order to keep our observations within a nonfluidized regime and for amplitudes going from the critical amplitude  $A_c$  up to amplitudes just below the amplitude at which bifurcation or period doubling starts to appear in each case. All the measurements were performed at a 5 cm depth (about the middle height of the granulate), and we waited for a couple of minutes before starting to measure allowing the convective flux to reach a stationary state. Ten independent measurements of the time it takes for a tracer to travel a fixed distance, or the convection velocity close to the wall ( $v_c$ ), were performed for each given condition of ampli-

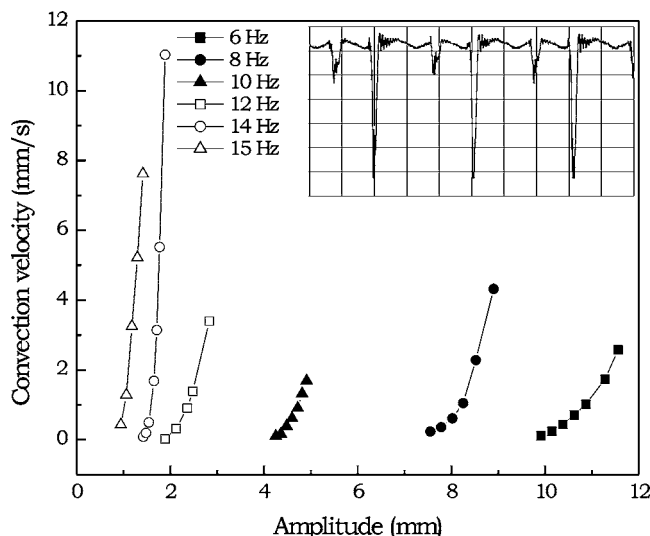


FIG. 2. Convection velocities as a function of the oscillation amplitude for six different frequencies. The inset shows the oscilloscope voltage signal from the inner piezo element. Two different times of flight are evident.

tude and frequency and excellent reproducibility was achieved. The results for the dependence of the convection velocity as a function of amplitude, for six different frequencies, are shown in Fig. 2. There the dependence of the convection onset on the frequency and a rapid increase of the convection velocity with the amplitude for a given frequency can be seen. It is worth noting that each curve starts at a different amplitude corresponding to its critical amplitude and they have different heights as well, this last point is due to the fact that we have omitted data at those amplitudes at which period doubling starts. The inset of Fig. 2 shows a typical signal from the piezo element placed at the bottom of the container for an amplitude well beyond the bifurcation. From the oscilloscope signal, the double period as well as the contrasting magnitude of the impacts at the end of short and long flights, respectively, are quite notorious. In order to perform a quadratic fit for each curve, first we have determined experimentally the critical amplitude of observing the appearance of a plateau on the bottom's piezo signal. Measurements of this critical amplitude with the naked ear registering the instant at which the system starts to make noise do not differ significantly from those made with the piezo element. These measurements are in agreement with the expected  $1/\omega^2$  dependence as can be seen in Fig. 3, in which the measured critical amplitude (squares) is shown. The circles represent extrapolations of the convection velocity quadratic fits to the point at which  $v_c$  vanishes. The continuous line was obtained using an  $\alpha/\omega^2$  function to fit the experimental data, with  $\alpha$  as a free parameter which depends on the static friction against the walls and the air pressure gradient. The influence of this last factors can be verified by comparing the continuous line with the dotted-dashed one (representing  $g/\omega^2$ ). It can be appreciated that the measured critical amplitude is larger than that of the ideal case in which opposition from frictional or dragging forces are not present.

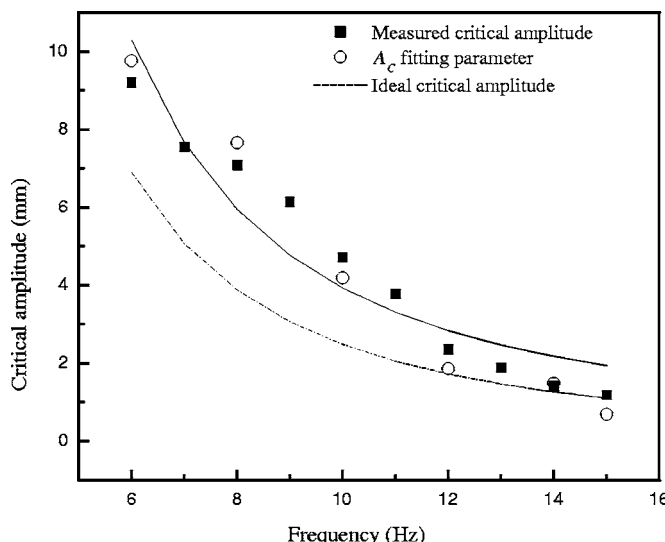


FIG. 3. Critical amplitudes as a function of frequency measured (squares) and extrapolated from the fitting procedure applied to the convection velocity curves shown in Fig. 2 (circles). The continuous line is a fit to the measured data showing the  $1/\omega^2$  dependence, and the dotted-dashed line represents the ideal  $g/\omega^2$  behavior.

Plotting the convection velocities against the squared excess amplitude, one gets a set of lines irradiated from the origin as can be seen in Fig. 4. In this figure, we show the parabolic dependence on the excess amplitude from which one could guess that the squared takeoff velocity or the kinetic energy of the granulate at takeoff causes the development of the convective flux. This *ansatz* for the dependence of convection velocity on the excess amplitude comes from the fact that the takeoff velocity is proportional to the maximum velocity acquired by the oscillating table which is  $A$  times  $\omega$ , and thus, the kinetic energy should scale with the squared amplitude. However, as we shall see, the dynamic quantity associated to the convective motion is the relative momentum between the bed and the container's walls, and not the kinetic energy of the bed measured from the laboratory's frame of reference, as one could naively guess at first glance. In order to establish the excess amplitude  $A_e$  as a dynamic parameter, we should write down the position, velocity, kinetic energy, and acceleration of the granulate relative to the vibrating plate and find out how  $A_e$  is related to these quantities.

From the frame of reference of the moving plate, the granulate acquires an increasing momentum relative to the container as the bed starts to lift up from the container's bottom. This is the onset of the distancing part of the shaking cycle. Once the granulate has reached its maximum distance from the bottom, the approaching part of the cycle begins. The shear stress is usually defined as a momentum transfer from one layer of a fluid to the layers in its vicinity. In our case, a momentum transfer from the wall to the bed takes place due to the relative motion between them and thus, the same definition applies. In other words, the container's walls exert a shear on the outermost cylindrical shell of the bed. The momentum associated to this shear is progressively transmitted to more inner shells creating a radial gradient of

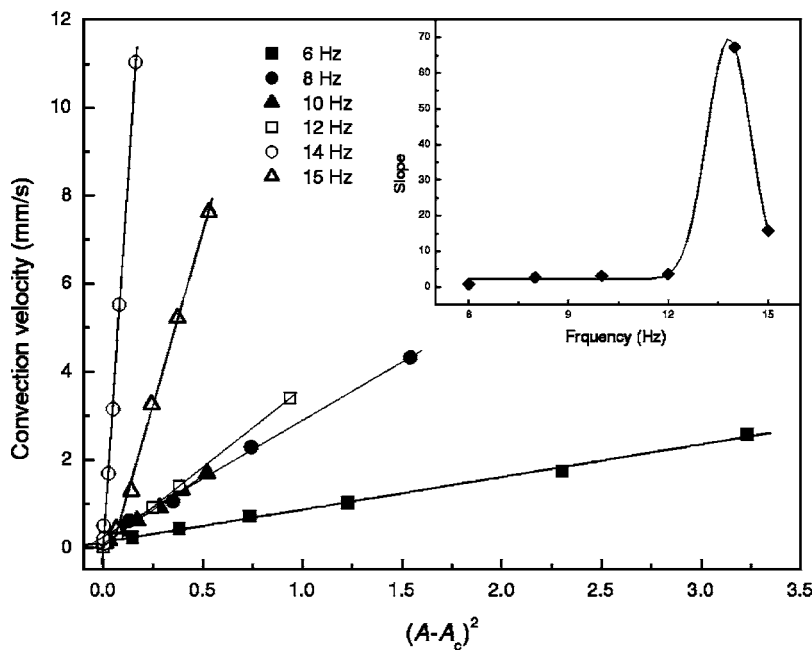


FIG. 4. Convection velocities as a function of  $A_e^2$ . Inset: Slopes of each straight line in the main figure plotted as a function of frequency.

distancing speeds. This is valid on both parts of the cycle, but during the distancing part, the packing is still quite compressed, exerting a strong pressure on the walls and allowing a more efficient momentum transfer or stronger shear. On the other hand, during the approaching part of the cycle, the packing is much looser (it has suffered decompaction by Reynolds dilatancy), and the shear friction is much less efficient, giving rise to a symmetry breakdown between both parts of the cycle. This leads to a net drag of the particles close to the walls in the direction in which they move (relative to the bed) during the distancing period and, consequently, to a net global convective flux. Experiments and simulations supporting this point of view were performed by Duran and co-workers [18], who studied the decompaction of a two-dimensional (2D) model granular system falling in a gravitational field. In their experiments, a 2D ordered column of discs is allowed to fall and the dynamics of the decompaction process is followed by high speed photography methods. There, one can clearly see, that as the granulate is more decompacted, its acceleration is closer to  $g$ . Moreover, for short times, the pressure exerted on the walls first grows for over an order of magnitude at positions where the density, or compaction, is large enough to allow the formation of arches (or contact chains) that span the container's width. For even longer falling times, the granulate is already too dilute near the walls, such that contact chains are not longer probable and thus, the pressure relaxes as it does the frictional shear efficiency. In our case, essentially the same phenomenology should occur despite the fact that the bed-bottom relative velocity changes its sign during the flight. For short times (the distancing part), the momentum transfer is more efficient, whereas, for larger times (the approaching part of the cycle), the bed is already too diluted so that the shear efficiency drops down giving rise to the nonsymmetrical shearing described above.

Following this description, the most relevant quantity is the average relative distancing velocity  $\langle v_d \rangle$  (not the kinetic

energy), which is a measure of the relative momentum, since the larger part of the momentum transfer takes place during this part of the cycle. It could be expected that the transferred momentum from the walls to the packing should be proportional to the relative momentum itself. To calculate  $\langle v_d \rangle$ , we first need to determine the time at which maximum distancing between the plate and the granulate is achieved.

Applying a Galileo transformation to  $z$  and  $\dot{z}$  for times larger than  $t_{to}$ , we obtain the required relative position and velocity of the granulate with respect to the oscillating plate

$$z' = -A \sin \omega t - \frac{g}{2}(t - t_{to})^2 + A_c + A\omega \sqrt{1 - \left(\frac{A_c}{A}\right)^2} (t - t_{to}), \quad (2)$$

$$\dot{z}' = A\omega \sqrt{1 - \left(\frac{A_c}{A}\right)^2} - g(t - t_{to}) - A\omega \cos(\omega t). \quad (3)$$

To find the ascension or distancing time ( $t_d$ ), we need to find the maximum of the relative position [Eq. (2)]. Equating to zero, Eq. (3) and solving for  $t$ , gives a transcendental equation that can be solved numerically. In order to get the average relative distancing velocity  $\langle v_d \rangle$ , we have to integrate Eq. (3) with respect to time between the lower limit  $t_{to}$  and the upper limit  $t_d$  (the time at which maximal separation is reached).

We have performed numerical evaluations of  $\langle v_d \rangle$  for the whole set of frequencies and amplitudes used in our experimental observations. The results are shown in Fig. 5, where the  $\langle v_d \rangle$  data are plotted as a function of the squared excess amplitude  $A_e^2$  for five different frequencies. The most striking feature in all cases is the linear growth of  $\langle v_d \rangle$  with  $A_e^2$ , which resembles the behavior of the convection velocity  $v_c$  itself. This could be interpreted as a signature of the underlying

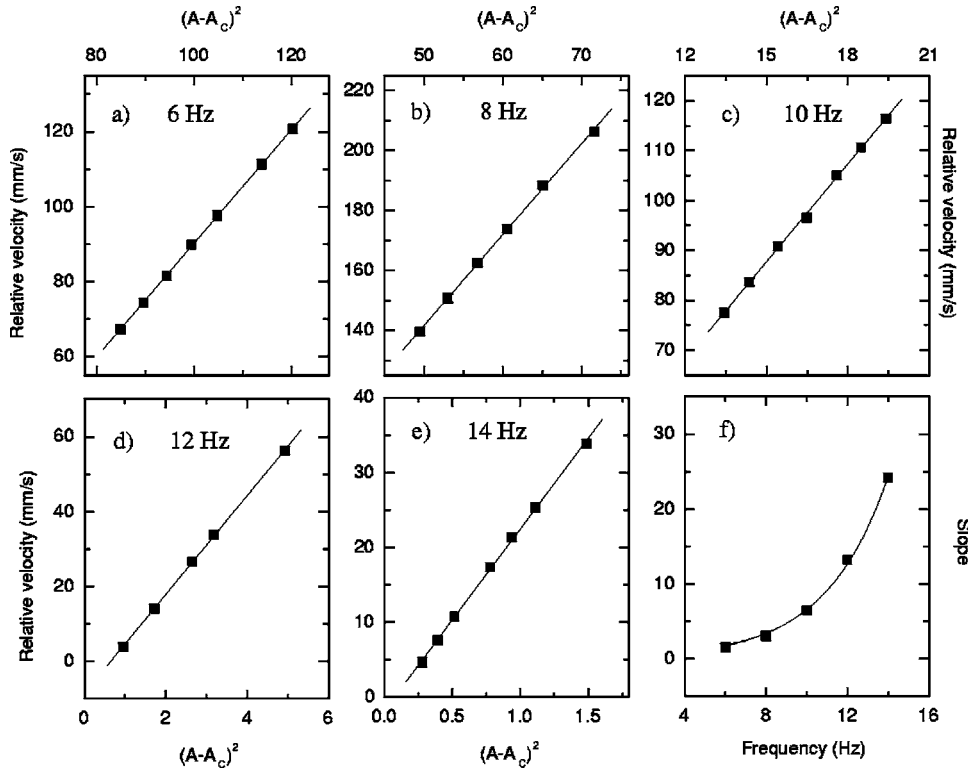


FIG. 5. In (a) to (e), average relative distancing velocity for five different frequencies are shown. In (f), the slopes of the previous graphics are plotted as a function of frequency.

mechanism that produces the convective streaming mode, which may be a shear proportional to the relative velocity between the granulate and walls during the distancing part of the cycle, as argued in the above discussion. In fact, in molecular dynamics simulations, it has been found that the shear stress is a monotonically increasing function of the moving wall velocity [19]—as can be expected—since the moving wall is transferring a momentum that should be proportional to its own speed. This study refers to continuous shearing under gravity but, due to the peculiar geometry involved in our experiment, it is hard to find rheological data more closely related to our own configuration in which the net of stresses in the bed is relaxed during the period of flight.

A second important issue is shown in Fig. 5(f) in which the slope of the previous graphics has been plotted as a function of frequency, where an exponential growth is shown by the continuous line fitted to the numerical data. For our experimental data, this has been done in the inset of Fig. 4, where the line, drawn just as a guide to the eye, shows a peak at 14 Hz. The fact that the frequency dependence found experimentally differs from the predicted by numerical explorations can be explained as a spontaneous symmetry breaking on the velocity field profile with frequency due to different normal modes of the whole vibrating system excited at different frequencies. In other words, the central heap that emerges as the convection starts moves toward the walls at increasing frequency making the local flux at the exploration region to decrease or increase depending on the net distance to the ascending flux axis in a complex way. This precludes the observation of the numerically predicted dependence on frequency, but does not affect the scaling with the excess amplitude, which in turn, is a clear signature

of a shear proportional to the mean velocity of the wall which exerts it. We should stress out that in molecular dynamics simulations, resonances as the one described above have been reported [10].

The Froude number or the dimensionless acceleration  $\Gamma$ , given as the maximum acceleration of the system divided by  $g$ , is extensively used to describe the behavior of granular materials under vertical shaking. However there is some controversy on the pertinence of this parameter [20], and several other parameters (as, for example,  $A$ ) have been proposed [5,21] in order to get a more physical insight into the system dynamics. As a matter of fact, the amplitude of the exciting movement gives a measurement of the initial velocity at which the granulate is thrown upward during a cycle with respect to the laboratory frame of reference, but is not appropriate to describe the shear force that leads to convection. Instead, we propose the excess amplitude, which is proportional to the average distancing velocity, as the dynamic parameter that should be used in experiments and simulations on the granular convection problem. In other words,  $\Gamma$  is a parameter related just to the plate but does not describe any of the relative dynamic quantities associated with the granulate's motion relative to the oscillating plate. Furthermore, the dimensionless character of  $\Gamma$  can be extended and the ratio of the excess amplitude to the critical amplitude ( $\Gamma - 1$ ) is proposed as a parameter proportional to the square root of  $\langle v_d \rangle$  and in turn to the net shear exerted on the granulate during an entire cycle.

Summarizing, we have shown that the average bed-plate distancing velocity scales with the squared excess amplitude as it does the convection speed close to the walls. This is strong evidence in favor of the hypothesis that shear drives convection through a momentum transfer from the walls to

the granulate which is proportional to the relative momentum between them. The shear stress exerted by the walls during the distancing part of the shaking cycle, produces an irreversible strain on the granulate that cannot be counterbalanced during the approaching period, due to the inherent hysteretic nature of dilatancy, leading to convection.

#### ACKNOWLEDGMENTS

We want to acknowledge the FAI program, IMP Grant No. FIES-98-101-I, CONACYT-U47611F, and the PROMEP PTC-UASLP-84 project for financial support. We thank A. Encinas and M. Ojeda for critical reading of the manuscript.

- 
- [1] J. Duran, T. Mazozi, E. Clément, and J. Rajchenbach, *Phys. Rev. E* **50**, 5138 (1994).
- [2] A. Garcimartín, D. Maza, J. L. Ilquimiche, and I. Zuriguel, *Phys. Rev. E* **65**, 031303 (2002).
- [3] S. R. Nagel, *Rev. Mod. Phys.* **64**, 321 (1992).
- [4] R. D. Wildman, J. M. Huntley, and D. J. Parker, *Phys. Rev. Lett.* **86**, 3304 (2001).
- [5] P. Philippe and D. Bideau, *Phys. Rev. Lett.* **91**, 104302 (2003).
- [6] R. Ramírez, D. Risso, and P. Cordero, *Phys. Rev. Lett.* **85**, 1230 (2000).
- [7] J. B. Knight, *Phys. Rev. E* **55**, 6016 (1997).
- [8] T. Shinbrot, D. Khakhar, J. J. McCarthy, and J. M. Ottino, *Phys. Rev. Lett.* **79**, 829 (1997).
- [9] J. B. Knight, E. E. Ehrichs, V. Y. Kuperman, J. K. Flint, H. M. Jaeger, and S. R. Nagel, *Phys. Rev. E* **54**, 5726 (1996).
- [10] J. A. C. Gallas, H. J. Herrmann, and S. Sokolowski, *Phys. Rev. Lett.* **69**, 1371 (1992).
- [11] E. L. Grossman, *Phys. Rev. E* **56**, 3290 (1997).
- [12] Y-h. Taguchi, *Phys. Rev. Lett.* **69**, 1367 (1992).
- [13] M. Bourzutschky and J. Miller, *Phys. Rev. Lett.* **74**, 2216 (1995).
- [14] J. Talbot and P. Viot, *Phys. Rev. Lett.* **89**, 064301 (2002).
- [15] Y. Nahmad-Molinari, G. Canul-Chay, and J. C. Ruiz-Suárez, *Phys. Rev. E* **68**, 041301 (2003).
- [16] M. E. Möbius, B. E. Lauderdale, S. R. Nagel, and H. M. Jaeger, *Nature (London)* **414**, 270 (2001).
- [17] D. A. Huerta and J. C. Ruiz-Suárez, *Phys. Rev. Lett.* **92**, 114301 (2004).
- [18] J. Duran, T. Mazozi, S. Luding, E. Clément, and J. Rajchenbach, *Phys. Rev. E* **53**, 1923 (1996).
- [19] P. A. Thompson and G. S. Grest, *Phys. Rev. Lett.* **67**, 1751 (1991).
- [20] T. Pöschel, T. Schwager, and C. Salueña, *Phys. Rev. E* **62**, 1361 (2000).
- [21] L. Vanel, A. D. Rosato, and R. N. Dave, *Phys. Rev. Lett.* **78**, 1255 (1997).